JOURNAL OF CATALYSIS 65, 281–296 (1980)

Surface Chemistry Models of Carbon Monoxide Oxidation on Supported Platinum Catalysts

RICHARD K. HERZ* AND SAMUEL P. MARIN†

* *Physical Chemistry Department and* † *Mathematics Department, General Motors Research Laboratories, Warren, Michigan 48090*

Received September 13, 1979; revised March 7, 1980

Rates of CO oxidation on noble metal catalysts are often represented by a Langmuir–Hinshelwood rate expression that assumes the competitive equilibrium adsorption of CO and O_2 on the active metal surface. Surface chemistry studies reported in the literature have shown, however, that this assumption cannot be justified under all conditions. As a result, the usual Langmuir–Hinshelwood rate expression is unable to explain the data of several reported studies of CO oxidation on Pt catalysts. In this report we develop two reaction models which include separate adsorption, desorption, and surface reaction steps, and which do not assume adsorption equilibrium. The ability of each model to fit CO oxidation rate data taken with an alumina-supported Pt catalyst is compared with that of the usual Langmuir–Hinshelwood rate expression. Unlike the usual rate expression, the surface chemistry models successfully simulate the abrupt transition in steady-state rate that occurs between the CO inhibition regime and the first-order regime. The parameter values used to fit the supported Pt data are similar to those determined with Pt crystals. However, they indicate that CO may be adsorbed less strongly on the supported Pt and that most of the surface Pt atoms in the supported catalyst were deactivated by an oxidizing pretreatment.

INTRODUCTION

Mathematical models of CO oxidation on supported noble metal catalysts usually account for the surface reaction with "bimolecular" Langmuir–Hinshelwood rate expressions similar to those shown in Eqs. (1) and (2).

$$\text{Rate} = \frac{kC_{CO}C_{O_2}}{(1 + K_{CO}C_{CO} + K_{O_2}C_{O_2})^2} \quad (1)$$

$$\text{Rate} = \frac{kC_{CO}}{(1 + K_{CO}C_{CO})^2} \quad (2)$$

Most studies of CO oxidation using supported Pt catalysts are carried out under conditions of relatively high gas phase CO concentration (C_{CO}) where these rate expressions can fit experimental data. However, they fail to predict the experimentally observed rapid transitions in steady-state rate from the CO inhibition regime (high C_{CO}) to the first-order regime (low C_{CO}). For example, Schlatter and Chou (*1*) observed these rapid transitions with a supported Pt catalyst at atmospheric pressure, and Golchet and White (*2*) observed similar behavior with Pt metal at low pressures (ca. 10^{-5} Pa).

The rate expressions (1) and (2) are obtained under the assumptions that the rate-determining step in the reaction is the surface reaction between adsorbed CO and adsorbed oxygen, and that the adsorption of CO always approaches equilibrium closely during the reaction. Studies of the surface chemistry of CO oxidation on unsupported noble metals, however, show that these assumptions do not apply under all conditions. The work of Golchet and White (*2*) with Pt, for example, shows that CO adsorption equilibrium is approached only at relatively high C_{CO}, where the rate-determining step is the adsorption of oxygen. The same work shows that, at low C_{CO}, the rate-determining step is the adsorption of CO and the surface concentrations of CO are much smaller than they would be if CO were in adsorption equilibrium.

0021-9517/80/100281-16$02.00/0

The purpose of the research described here is to develop a mathematical model of CO oxidation on supported Pt catalysts that represents the surface chemistry of this reaction system more accurately than the Langmuir–Hinshelwood expression does. Our development starts with the hypothesis that the Pt in a supported catalyst acts in CO oxidation like the surface Pt in metal samples used in surface chemistry studies. In our development, we make no assumptions about which reaction step is rate determining and do not assume adsorption equilibrium for CO. Here, we present two models to compare their predictions with those of Eq. (2) by fitting experimental data collected by Schlatter and Chou (*1*) for a supported Pt system. Whenever possible, we use parameter values taken from surface chemistry studies of unsupported Pt to fit supported Pt data.

METHODS

The procedure we have used in developing our reaction models is outlined below:

(1) Identify the surface species and the reaction steps in the mechanism of CO oxidation on Pt.

(2) Develop expressions for the rates of each of these reaction steps and write conservation equations for the surface species.

(3) Solve the conservation equations for surface concentrations under steady-state conditions and compute the reaction rate.

(4) Compare predicted rates to measured rates, taking into account the possible presence of diffusional limitations in supported catalysts.

After a discussion of the reaction mechanism, we define dimensionless surface concentrations and develop adsorption rate expressions. Two reaction models are then presented. In the last part of the Methods section we discuss corrections for the effects of diffusional limitations. The procedure used to solve the conservation equations is presented in Appendix 2.

Reaction Mechanism

The primary reaction that occurs during the catalytic oxidation of CO on noble metals is the reaction of relatively tightly adsorbed oxygen atoms with adsorbed CO molecules which are highly mobile on the catalyst surface. Recent work, for example, that of Ertl with Pd (*3, 4*) and Matsushima with Pt (*5, 6*), shows that the participation of a classical Eley–Rideal mechanism involving gas phase CO is unlikely. Adsorbed oxygen atoms are formed as a result of the adsorption and then the dissociation of molecular oxygen (*7–9*). Participation of oxygen in the reaction through the formation and reduction of a metal oxide can be ruled out for Pt and Pd at temperatures below 573 K (*3, 10*). Surface oxides can form on Pt metals during high temperature treatment in oxygen (e.g., in a pretreatment step), but the "oxide" oxygen is very strongly bound and cannot be removed by CO at the reaction temperatures considered here (<573 K) (*11*). Transient oxidation and reduction processes, however, may be a factor in the activity instabilities that have been observed during CO oxidation (*12*). Once formed, CO_2 does not interact with the metal surface (*3*). The mechanism of CO oxidation on Pt, then, can be represented by the following chemical equations:

$$CO \underset{2}{\overset{1}{\rightleftarrows}} CO_a \qquad (3)$$

$$O_2 \underset{3b}{\overset{3a}{\rightleftarrows}} O_{2-a} \qquad (4)$$

$$O_{2-a} \underset{3d}{\overset{3c}{\rightleftarrows}} 2O_a \qquad (5)$$

$$CO_a + O_a \overset{4}{\rightarrow} CO_2 \qquad (6)$$

The subscript a refers to species adsorbed on the Pt surface, while CO, O_2, and CO_2 are gas phase species.

In the present work we are interested only in reaction temperatures below 573 K where the rate of association of oxygen

atoms is negligibly slow (*7*), thus we may neglect reaction 3d. Two assumptions allow us to simplify the system further:

(1) O_{2-a} and O_2 are in adsorption equilibrium, and

(2) the surface concentration of O_{2-a} is negligibly small.

Assumption (1) is reasonable in view of the low sticking probability of oxygen on Pt, about 0.01 to 0.1 (*7*), which indicates that the rate of O_2 dissociation (reaction 3c) is slow compared with the rate of O_2 desorption (reaction 3b). Assumption (2) is reasonable since molecular O_2 is adsorbed weakly on Pt (*8, 9*). These assumptions make it unnecessary to consider O_{2-a} explicitly and allow reactions 3a, 3b, and 3c to be represented by one complex reaction, the dissociative adsorption of oxygen.

Under the above conditions, the mechanism of CO oxidation on Pt can be represented by:

$$CO \underset{2}{\overset{1}{\rightleftarrows}} CO_a \qquad (7)$$

$$O_2 \xrightarrow{3} 2O_a \qquad (T < 573\ K) \qquad (8)$$

$$CO_a + O_a \xrightarrow{4} CO_2 \qquad (9)$$

This is the set of reactions considered in the development of our reaction models.

Surface Concentrations

We will write surface rate and conservation equations in terms of dimensionless surface concentrations. In doing so, we assume that

(1) adsorbed species are distributed randomly over the metal surface, and

(2) average properties of the metal surface can be used to describe its catalytic behavior.

Reaction of CO_a and O_a at the boundaries of islands of one of these species may be important under some conditions on the surfaces of bulk metals (*3, 6*). The formation of adsorbate islands may be less probable on the very small metal crystallites in supported catalysts, however, and we feel that it is unnecessary to include this complication here. Metal atoms on a support are grouped in crystallites with a distribution of sizes, and a metal atom may be arranged with other atoms in a variety of configurations. As a result, the catalyst surface may possess sites with a distribution of adsorption properties and activities (*16*). We regard the values of model parameters that fit experimental data as estimates of average properties of the catalyst.

Dimensionless surface concentrations are defined as follows:

$$\theta_{CO} = \left(\frac{\text{No. of } CO_a}{\text{No. of surface metal atoms}}\right) \qquad (10)$$

$$\theta_O = \left(\frac{\text{No. of } O_a}{\text{No. of surface metal atoms}}\right). \qquad (11)$$

The use of the number of surface metal atoms in the system (a constant) as the normalizing factor in (10) and (11) is not meant to imply that a CO molecule or oxygen atom bonds directly to one metal atom. The detailed structures of the bonds between adsorbed species and metal atoms are not explicitly considered in this development. Instead, we develop a set of assumptions concerning the occupation of the Pt surface by CO_a and O_a and use these assumptions to describe the manner in which adsorption rates depend on the dimensionless surface concentrations.

We first point out that a ratio of one adsorbed CO molecule to one surface Pt atom is often used in the determination of metal areas in supported Pt catalysts (*17*). This suggests that the maximum value of θ_{CO} is 1.0 for supported Pt. Next we note that a ratio of one adsorbed oxygen atom to two surface metal atoms has been found for chemisorption on highly dispersed, supported Pt (*17, 18*). This leads to our assumption that the maximum value of θ_O is 0.5 for the supported Pt catalyst considered here. The maximum values of $\theta_{CO} = 1.0$ and $\theta_O = 0.5$ are also suggested by studies

(*3*, *9*, *19*) of chemisorption of large Pt and Pd crystals. The major effect on our models' predictions of a change in the maximum value of θ_0 assumed would be a change in the apparent order of the reaction in CO at low gas phase CO concentrations.

The limiting values of θ_{CO} and θ_0 given above can be obtained from the following assumptions:

(1) A CO_a excludes other CO_a from an area on the surface equivalent in size to the area occupied by one surface Pt atom.

(2) An O_a excludes other O_a from an area on the surface equivalent in size to the area occupied by two surface Pt atoms.

The coadsorption and coexistence of CO_a and O_a on Pt is difficult to study because of the high reactivity of this system. Experimental studies using Pt metals have shown that a surface saturated with respect to oxygen adsorption by O_a can still adsorb CO, while a surface saturated with CO_a cannot adsorb oxygen (*4*). The preceding statements are qualitatively consistent with the following additional assumptions:

(3) A CO_a excludes O_a from an area on the surface equivalent in size to the area occupied by one surface Pt atom.

(4) An O_a excludes CO_a from an area on the surface equivalent in size to the area occupied by one surface Pt atom.

We also assume that CO will adsorb randomly on the available area of a surface populated with O_a. An alternate description of the coadsorption of CO and oxygen is considered below in a discussion of the surface concentration dependence of the rate of CO adsorption.

Adsorption Rate Expressions

The rate of adsorption of CO or oxygen on the surface of a metal crystallite in a catalyst micropore is jointly proportional to

(1) the rate at which gas phase CO or O_2 molecules collide with the metal surface, and

(2) the probability that a CO or O_2 molecule striking the surface will adsorb as CO_a or O_a. This probability is taken to be equal to the product of

(i) an initial sticking coefficient, the probability that the molecule will adsorb or "stick" when it strikes a bare metal surface, and

(ii) a term that describes the dependence of the rate of adsorption on the surface concentrations of CO_a and O_a.

The rate of collision of gas phase CO or O_2 molecules with the metal surface is expressed below as a collision frequency, $F(s^{-1})$.

$$F_{CO} = (RT_g/2\pi M_{CO})^{1/2}\sigma C_{CO} \qquad (12)$$

$$F_{O_2} = (RT_g/2\pi M_{O_2})^{1/2}\sigma C_{CO}. \qquad (13)$$

These expressions were obtained under the assumption of ideal gas behavior. The gas temperature, T_g, is assumed to equal the catalyst temperature, T. R is the ideal gas constant, M is molecular weight, and C is gas phase concentration with the dimensions (mol cm^{-3}). The coefficient σ is the area occupied by 1 mol of surface metal atoms (cm^2 mol^{-1}).

The initial sticking coefficients for CO and O_2 are S_{CO} and S_{O_2}, respectively. These are the probabilities that one of these molecules will adsorb when it collides with a bare metal surface. The expression $(S_{O_2}K_3 \exp[-\Delta E_3/RT])$ is the probability that an oxygen atom in an O_2 molecule impinging on a bare surface will adsorb as O_a, under the conditions given above for reaction (3). This expression is the initial sticking coefficient for oxygen atoms, S_O:

$$S_O = (S_{O_2}k_3 \exp[-\Delta E_3/RT]). \qquad (14)$$

The preexponential factor and the apparent activation energy for the complex reaction (3) are composed of k's and ΔE's for the reactions (3c) and (3b):

$$k_3 = (k_{3c}/k_{3b}) \qquad (15)$$

$$\Delta E_3 = (\Delta E_{3c} - \Delta E_{3b}). \qquad (16)$$

Since k_3 is a ratio of two preexponential factors, it is dimensionless. The energy difference ΔE_3 can appear to be a "negative activation energy" if ΔE_{3b} is greater than ΔE_{3c}. S_{CO} is assumed to have no temperature dependence.

In both reaction models we assume that the rate of adsorption of CO is proportional to the probability that a CO molecule strikes the metal surface at an area where adsorption of CO is not excluded by CO_a or O_a. Using the assumptions stated in the previous section, this probability is

$$(1 - \theta_{CO} - \theta_O). \tag{17}$$

This surface concentration dependence is an approximation to experimentally observed behavior. In the absence of oxygen, the rate of adsorption of CO on Pt has been observed to remain constant as θ_{CO} increases from 0.0 to about 0.25 to 0.5 before the rate decreases as θ_{CO} increases further (*19*). Evidently, CO adsorption involves a mobile precursor state in which an impinging CO molecule can find an open adsorption area some distance from its point of impact with the surface (*20*). Preadsorbed oxygen on Pd(111) (*3, 4*) and Ir(100) (*21*) has been found to not inhibit the rate of CO adsorption. This behavior can be explained by precursor adsorption of CO on a surface where θ_O is 0.5 or less, or by independence of oxygen and CO adsorption sites to the extent that CO molecules do not interact with preadsorbed O_a. The precursor explanation seems to be more likely in the case of Pd(111), where rather intricate interactions between CO_a and O_a were observed. The major effect on our models' predictions of the inclusion of a term in (17) to account for precursor adsorption, or the deletion of the θ_O term, would be to make the rate of CO oxidation more nearly first order in CO at low CO pressures.

In Model I we assume that the rate of dissociative adsorption of oxygen is proportional to the probability that an O_2 molecule strikes the metal surface at an area where the adjacent adsorption of two oxygen atoms is not excluded by CO_a or O_a. This probability is equal to the square of the fraction of the surface that is available for adsorption of one O_a under the assumptions given in the preceding section:

$$(1 - f\theta_{CO} - 2\theta_O)^2, \tag{18}$$

where

$$f = \left(\frac{1 - 2\theta_O}{1 - \theta_O}\right). \tag{19}$$

The term $f\theta_{CO}$ represents the CO_a that are not immediately adjacent to O_a and thus that are excluding oxygen adsorption from areas not accounted for by the $2\theta_O$ term. Reaction Models I and II differ only in the surface concentration dependence assumed for the rate of oxygen adsorption. The dependence assumed in Model II is

$$(1 - f\theta_{CO} - 2\theta_O)(1 - 2\theta_O). \tag{20}$$

Our reason for considering (20) is discussed below.

The expressions (18) and (20) affect the results presented below primarily through their simple dependence upon θ_{CO} at low θ_O: as θ_O approaches zero, the rate of oxygen adsorption is proportional to $(1 - \theta_{CO})^2$ in Model I and is proportional to $(1 - \theta_{CO})$ in Model II.

Reaction Model I

The expressions used in Model I for the rates, $r(s^{-1})$, of reactions 1 through 4 are listed below.

$$r_1 = F_{CO}S_{CO}(1 - \theta_{CO} - \theta_O) \tag{21}$$

$$r_2 = k_2 \exp[-(\Delta E_2 - \beta\theta_{CO})/RT]\theta_{CO} \tag{22}$$

$$r_3 = 2F_{O_2}S_O(1 - f\theta_{CO} - 2\theta_O)^2 \tag{23}$$

$$r_4 = k_4 \exp[-\Delta E_4/RT]\theta_{CO}\theta_O. \tag{24}$$

We specify that our system is isothermal. The k's are preexponential factors with dimension (s^{-1}) and the ΔE's are activation energies. Note the coefficient β in Eq. (22) which causes the activation energy for desorption of CO to vary with the surface concentration of CO. This surface concen-

tration dependence is often used when thermal desorption curves are fit (*22, 23*) and is related physically to the mutual interaction of adsorbed CO molecules (*24*).

Conservation equations for the surface species CO_a and O_a follow.

$$\frac{d\theta_{CO}}{dt} = r_1 - r_2 - r_4 \quad (25)$$

$$= F_{CO}S_{CO}(1 - \theta_{CO} - \theta_O) - k_2 \exp[-(\Delta E_2 - \beta\theta_{CO})/RT]\theta_{CO} - k_4 \exp[-\Delta E_4/RT]\theta_{CO}\theta_O \quad (26)$$

$$\frac{d\theta_O}{dt} = r_3 - r_4 \quad (27)$$

$$= 2F_{O_2}S_O(1 - f\theta_{CO} - 2\theta_O)^2 - k_4 \exp[-\Delta E_4/RT]\theta_{CO}\theta_O. \quad (28)$$

The rate of CO oxidation expressed as a turnover frequency is:

$$\text{Rate}(s^{-1}) = k_4 \exp[-\Delta E_4/RT]\theta_{CO}\theta_O. \quad (29)$$

This rate is the average number of CO_2 molecules produced per active metal atom in the system per second.

Equations (26) and (28) must be solved for θ_{CO} and θ_O at a specified T, C_{CO}, and C_{O_2} in order to calculate the rate. In this study we have calculated the rate under steady-state conditions where the time derivatives in (26) and (28) equal zero. These equations can also be used to model the reaction system under transient conditions. The solution procedure used to solve the conservation equations for Models I and II is described in Appendix 2.

Models similar to this one, describing the mechanism given in Eqs. (7)–(9) with the addition of a classical Eley–Rideal step involving gas phase CO, have been used by many researchers to explain their results qualitatively or analytically to fit limiting behavior in various operating regimes: in particular, we would like to refer the reader to the discussion by White and co-workers (*13*). A numerical solution of a set of equations corresponding to reactions 2, 3, and 4 was used by Bonzel and Burton (*14*) to fit the results of the temperature-programmed reaction of preadsorbed CO with gas phase O_2 on Pt(110). Recently, Strozier *et al.* (*15*) have presented numerical solutions of a model describing this mechanism plus an Eley–Rideal step.

None of the above works discussed the multiple solutions for rate and surface concentration which are possible under some conditions with this type of model, although Golchet and White (*2*) experimentally observed more than one "meta-stable" rate at a given CO concentration over Pt foil in high vacuum. Wicke and co-workers (*25*) showed qualitatively how rate multiplicities could exist with a model of CO oxidation in which the rate of oxygen adsorption is proportional to $(1 - \theta_{CO})^2$. Eigenberger (*26, 27*) followed up Wicke's proposals with a mathematical analysis of Langmuir-type kinetic equations in which adsorption equilibrium was not assumed, and discussed rate multiplicities and instabilities. When considering the application of his analysis to CO oxidation, Eigenberger used a rate expression which described the simultaneous reactions of two adsorbed CO molecules with an adsorbed O_2 molecule and assumed that O_2 was in adsorption equilibrium. Bykov and co-workers (*28, 29*) have made an analysis of the multiplicities and dynamics of a CO oxidation reaction model representing the mechanism of Eqs. (7)–(9), also allowing the association of O_a and desorption of O_2 at high temperatures and including the Eley–Rideal step in some cases.

Reaction Model II

In Model II we specify that the rate of reaction 3, the dissociative adsorption of oxygen, is given by

$$r_3 = 2F_{O_2}S_O(1 - f\theta_{CO} - \zeta_O)(1 - 2\theta_O). \quad (30)$$

Oxygen adsorption is less strongly inhibited by adsorbed CO in Model II than it is in Model I.

We introduce Model II because Model I appears to predict too great a decrease in

reaction rate with increasing C_{CO} when adsorption parameters determined with Pt crystals are used to fit supported Pt data. This is certainly not a reason to reject Model I since we do not know yet how similar the Pt is in the two types of catalysts. The adsorption area requirements for oxygen which were assumed in Model I are reasonable for adsorption on low index surfaces of large metal crystals. We suggest two cases in which the apparent inhibition of oxygen adsorption by CO_a would be less than that obtained with Model I:

(1) The adsorption area requirements are the same as in Model I, but inhibition by CO_a is reduced by the action of a mobile precursor state in oxygen adsorption, in a manner similar to that mentioned above for CO adsorption.

(2) The area requirements for adsorption on the surfaces of very small crystallites are different from those which are reasonable for low index surfaces.

A reaction model similar to II could also be obtained with a different reaction mechanism in which CO reacts with an adsorbed oxygen molecule to form CO_2 and an adsorbed oxygen atom, the oxygen atom formed when reacting immediately with another CO molecule. This reaction mechanism was considered by Cochran *et al.* (*30*) in study of CO oxidation on a supported Pt catalyst.

The conservation equation for O_a in Model II is:

$$\frac{d\theta_O}{dt} = 2F_{O_2}S_O(1 - f\theta_{CO} - 2\theta_O)(1 - 2\theta_O) - k_4 \exp[-\Delta E_4/RT]\theta_{CO}\theta_O. \quad (31)$$

The conservation of CO_a and the rate of CO oxidation are again given by Eqs. (26) and (29), respectively.

Correction for Diffusional Limitations

When diffusional limitations are present in a supported catalyst during CO oxidation experiments in excess O_2, the gas phase CO concentration and thus the reaction rate varies across the interiors of the catalyst pellets. However, only the overall rate and the gas phase CO concentration around the outside of the pellets can usually be measured. This means that a rate calculated using a given C_{CO} must be multiplied by an effectiveness factor to compare it with the overall rate measured at this concentration.

Below we fit data taken using a supported Pt catalyst whose properties are listed in Table 1. We used these properties to estimate effectiveness factors for the two surface chemistry models and the Langmuir–Hinshelwood rate expression. Because only a thin outer layer of the spherical pellets was impregnated with Pt, slab geometry was assumed.

In the low C_{CO} regime, our models predict that the rate is approximately first-order in C_{CO}. To estimate an effectiveness factor, we first calculated a pseudo first-order rate constant, k, at any C_{CO} in the low C_{CO} regime using the rate predicted by the model.

$$k(\text{cm s}^{-1}) = \frac{\text{Rate(mol cm}^{-2}\text{ s}^{-1})}{C_{CO}(\text{mol cm}^{-3})} \quad (32)$$

The conversion of rates from turnover frequencies to specific rates in terms of (mol cm^{-2} s^{-1}) is discussed in the beginning of the Results section. Next, the Thiele parameter ϕ was calculated using the values of the parameters L, a, and D given in Table 1.

$$\phi = L(ka/D)^{1/2}. \quad (33)$$

The effectiveness factor η is (e.g., (*31*))

$$\eta = (\tanh \phi)/\phi, \quad (34)$$

and

$$\text{Rate}_D = (\text{Rate} \cdot \eta). \quad (35)$$

Rate_D is the predicted rate which can be compared to the experimental rate. The effects of diffusional limitations were estimated to be minimal in the higher range of C_{CO} in which data were taken as a result of relatively low reaction rates and high CO

TABLE 1

Catalyst Properties

Catalyst: Pt on γ-alumina[a]	
Pellet diameter (cm)	0.34
Pellet density (g cm^{-3})	1.2
BET surface area (cm^2 g^{-1})	2.3×10^6
Ave. macropore radius (cm)	5.0×10^{-5}
Ave. micropore radius (cm)	1.2×10^{-6}
Ave. macropore volume (cm^3 g^{-1})	0.2
Ave. micropore volume (cm^3 g^{-1})	0.4
Pt loading (wt%)	0.036
Pt impregnation depth (cm)	3.9×10^{-3}
Pt surface area (cm^2 g^{-1}) (by CO chemisorption)	7.5×10^2
Pt dispersion	0.81
Pretreatment procedure	
At 773 K: 10 min in He, 60 min in H_2, 10 min in He, 10 min in O_2, 10 min in He; cool in He	
Parameters used to estimate effectiveness factors	
Characteristic diffusion length, L(cm) (impregnation depth)	3.9×10^{-3}
Local loading in impregnated region, a (cm^2 cm^{-3})	2.7×10^4
Effective diffusivity for CO at 473 K, D (cm^2 s^{-1})	2×10^{-2} (*33*)

[a] Prepared by impregnation of pellets with H_2PtCl_6.

concentrations (*1*).

$Rate_D$ for the Langmuir–Hinshelwood expression was estimated using effectiveness factors computed by Wei and Becker (*32*) for a diffusion–reaction system in which the intrinsic rate is given by Eq. (2).

RESULTS

Comparison with Experimental Data

Model I, when used with realistic values of adsorption and reaction parameters for Pt crystals, can semiquantitatively fit data reported for CO oxidation on bulk Pt at low pressures. For example, the model can duplicate the abrupt transition in rate with CO pressure and some features of the "meta-stable states" reported by Golchet and White (*2*). A direct fit of CO oxidation kinetic data over the supported Pt catalyst considered here is not possible with either model using the parameter values determined from experiments with Pt crystals. This result is not surprising: the adsorption properties and activities of metal atoms dispersed on an oxide support can be expected to differ from those of metal atoms in the surface layer of a large crystal. One possibility is that not all of the surface Pt atoms in this supported catalyst were active. Let us introduce the parameter α, the fraction of the surface metal atoms in a supported catalyst that are active for CO oxidation. Rate parameters and surface concentrations now refer only to properties of the active surface. Now the reaction rate can be expressed as

$$\text{Rate}(\text{mol cm}^{-2}\ \text{s}^{-1}) = \left(\frac{\alpha}{\sigma}\right) k_4 \exp[-\Delta E_4/RT]\theta_{CO}\theta_O, \quad (36)$$

the rate per cm^2 of noble metal determined by chemisorption measurements.

In Fig. 1 we compare the predictions of our models with those of Eq. (2) by fitting rate data taken by Schlatter and Chou (*1*). Table 1 lists the properties of their supported Pt catalyst. Table 2 lists the parame-

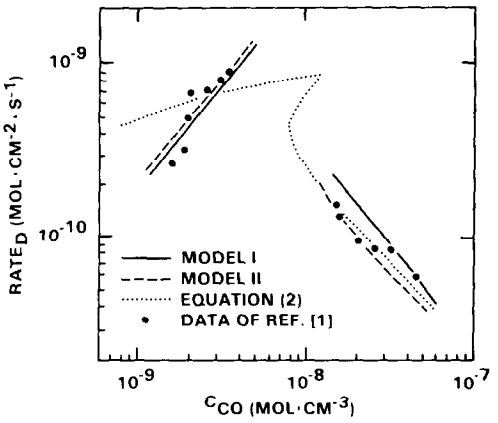

FIG. 1. CO oxidation rate in 1% O_2 (2.6×10^{-7} mol cm^{-3}) at 1 atm total pressure and 473 K. The predictions of Models I and II and Eq. (2) are corrected for the effects of diffusional limitations. The parameter values used in Eq. (2) are: k = 43.8 cm s^{-1}, K_{CO} = 4.36×10^9 cm^3 mol^{-1}.

ter values used in Models I and II and the corresponding values for a Pt(111) surface. The data points in Fig. 1 are measurements of rates of CO oxidation in an external recycle reactor.

The predictions of Eq. (2) and both models have been corrected for the effects of diffusional limitations. Note the multiple rate solutions at a given intermediate C_{CO} that are predicted by this fit of Eq. (2) to the data. These rate multiplicities result from a complex interaction between the processes of diffusion and reaction (*32, 33*). Obviously, the data presented are not sufficient to show either the presence or absence of multiplicities. Predictions of Models I and II are not shown at intermediate C_{CO} because the effects of diffusional limitations are not easily estimated there. In a future report we will discuss the incorporation of our reaction models into a single pellet diffusion and reaction model.

Both surface chemistry reaction models do a better job of fitting the rate data in the low C_{CO} regime than the Langmuir–Hinshelwood expression does. Using the pa-

TABLE 2

Parameter Values Used in Reaction Models I and II

Parameter	Pt/Al_2O_3 catalyst (Table 1)		Pt(111)	
	Model I	Model II		
α	1.77×10^{-4}	1.77×10^{-4}	—	
σ(cm^2 mol^{-1})	4.03×10^8	4.03×10^8	4.03×10^{8a}	
Reaction 1				
S_{CO}	0.5	0.5	0.5 (*20*)	
Reaction 2				
k_2(s^{-1})	6.72×10^{14}	3.4×10^{13}	1.0×10^{13}	(*19*)
ΔE_2(kJ mol^{-1})	124	124	124	(*19*)
β(kJ mol^{-1})	27.2	27.2	27.2	(*19*)
Reaction 3				
S_0 (473 K)	0.012	0.006	0.012	(*8, 9*)[b]
S_{O_2}	1.0	1.0	1.0	(*8, 9*)[b]
k_3	4.04×10^{-3}	2.02×10^{-3}	4.04×10^{-3}	(*8, 9*)[b]
ΔE_3(kJ mol^{-1})	−4.2	−4.2	−4.2	
Reaction 4				
k_4(s^{-1})	1.0×10^{13}	1.0×10^{13}	*c*	
ΔE_4(kJ mol^{-1})	56.5	56.5		

[a] Calculated using a Pt atomic radius of 1.39×10^{-8} cm.

[b] S_0 (473 K) extrapolated from S_0 (200 K) = 0.05 (*8, 9*) using $\Delta E_3 = -4.2$ kJ mol^{-1} (*8, 9*); S_{O_2} = 1.0 assumed; k_3 based on these S_0, ΔE_3, and S_{O_2}.

[c] Values of k_4 and ΔE_4 selected to make the rate constant of the surface reaction fast with respect to the rate constant of CO desorption as indicated by the data of Refs. (*2, 13*). Model predictions are insensitive to changes in these values of k_4 and ΔE_4.

rameter values listed in Table 2, the models predict that CO is not in adsorption equilibrium in the low C_{CO} regime, while the Langmuir–Hinshelwood expression is based on an assumption of adsorption equilibrium.

The parameter values for the two surface chemistry models were not optimized to give best fits. Apparently, the models can be made to fit these data equally well.

With the exception of α and k_2, the values of the parameters used in the models to fit the supported Pt data are similar to those determined with bulk, unsupported Pt (see Table 2). The values of k_4 and ΔE_4 were chosen to make the surface reaction constant, $k_4 \exp[-\Delta E_4/RT]$, large relative to the rate constant for CO desorption. We did this because we can model the data of Golchet and White (*2*) only by using a large reaction rate constant. The value of k_4 was arbitrarily set to 10^{13} s^{-1}; it is probably lower since the reaction is bimolecular. Increasing the reaction rate constant (by decreasing ΔE_4, for example) has a minor effect on the predictions of the models. We had to increase the value of the rate constant for CO desorption in both models from that determined in Pt crystal studies. We chose to do this by increasing k_2 since the data were taken at only one temperature. This modification indicates that CO may be less strongly bound to the supported Pt than to Pt(111). The sticking coefficient for oxygen in this fit of Model II is less than the Pt(111) value. The small values of α were most surprising. They indicate that only a small fraction of the surface atoms in this catalyst were active. In the Discussion section we ascribe the small value of α to the effect of the severe oxidizing pretreatment given to this catalyst (see Table 1).

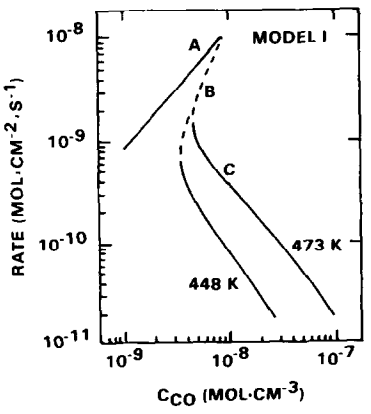

FIG. 2. Model I: CO oxidation rate in 1% O_2 (2.6×10^{-7} mol cm^{-3}) at 1 atm total pressure. No corrections for the effects of diffusional limitations are made. In Model I, the rate of dissociative adsorption of oxygen is proportional to $(1 - \theta_{CO})^2$ as θ_O approaches zero.

Below, we discuss the behavior of the two surface chemistry models in more detail.

Reaction Model I

Figure 2 shows the rate predictions of Model I at two different temperatures. No corrections for diffusional effects are made in this figure. The reaction rate varies only slightly with temperature at low C_{CO} where the reaction rate is limited by the rate of adsorption of CO molecules. A much stronger variation in rate with temperature is present at higher C_{CO}, where the reaction is limited by the rate of adsorption of oxygen on a surface with a high concentration of CO_a. This behavior was observed by Golchet and White (*2*) using Pt foil and by Schlatter and Chou (*1*) using a supported Pd catalyst. The dimensionless surface concentrations θ_{CO} and θ_O predicted by the model are shown as a function of C_{CO} in Fig. 3. Curve segments A, B, and C in the surface concentration plots correspond to curve segments with the same labels in the rate plot.

At low C_{CO} the metal is partially covered with oxygen atoms and the reaction rate is limited by the adsorption rate of CO molecules: every adsorbing CO molecule reacts rapidly so θ_{CO} is low. As C_{CO} is increased the rate increases and θ_O decreases. At the rate maximum, the adsorption rate of CO molecules equals the maximum adsorption rate of oxygen atoms at constant C_{O_2}, and

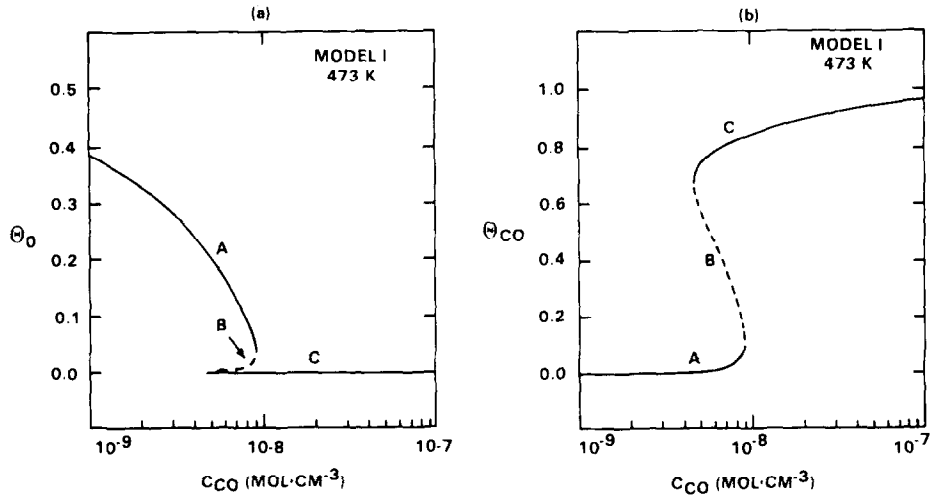

FIG. 3. Model I: Dimensionless surface concentrations of (a) $O_a(\theta_O)$ and (b) $CO_a(\theta_{CO})$ under the reaction conditions of Fig. 2 at 473 K.

both θ_O and θ_{CO} are low. With a further increase in C_{CO}, more CO molecules can adsorb than oxygen atoms and CO accumulates, inhibiting the adsorption of oxygen and decreasing the reaction rate. At high C_{CO}, θ_{CO} is high, θ_O is low, and the reaction rate is limited by the adsorption rate of oxygen.

Note that in the range of C_{CO} that curve segment B spans there are three solutions to the kinetic model at a given C_{CO}, while unique solutions exist at other concentrations. Wicke (*25*) has given a physical explanation of multiplicities in this type of model. Multiple solutions can exist when the rate constant for the surface reaction is large with respect to the rate constant for CO desorption. The presence of multiple solutions is not a necessary result of this model: only unique solutions are obtained when the surface reaction rate is low enough so that equilibrium adsorption of CO is approached, or at higher temperatures where the rate of CO desorption becomes large.

The surface concentrations and the reaction rate which will be present at intermediate C_{CO}, in the system that is represented by the curves in Figs. 2 and 3, will depend upon the recent history of the system. For example, if C_{CO} starts out low and then is increased, the system will move along the curves to the right until the junctions between the A and B curves are reached. Then, the system will jump to the points on the C curves that lie at the C_{CO} corresponding to the AB junctions. Further increases in C_{CO} will move the system to the right along the C curves. As C_{CO} is decreased from a high level, the system will move to the left along the C curves until the CB junctions are reached and then will jump to the corresponding points on the A curves. We have made the B curve segments dashed because these states of the system would be hard to reach experimentally and would be unstable even if they could be reached.

Reaction Model II

The rate and surface concentration predictions of Model II are shown in Figs. 4 and 5. The behavior of this model is similar to that of Model I except at intermediate C_{CO}, where rate and surface concentration multiplicities do not exist with Model II. Both models predict rapid transitions in rate and surface concentration with small changes in the intermediate levels of C_{CO}. Like Model I, Model II predicts a relatively

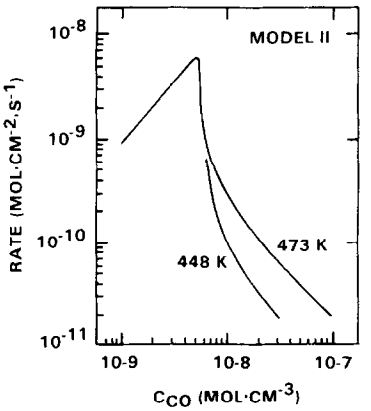

FIG. 4. Model II: CO oxidation rate in 1% O_2 (2.6×10^{-7} mol cm^{-3}) at 1 atm total pressure. No corrections for the effects of diffusional limitations are made. In Model II, the rate of dissociative adsorption of oxygen is proportional to $(1 - \theta_{CO})$ as θ_O approaches zero.

large apparent activation energy for the rate at high C_{CO} and a small apparent activation energy at small C_{CO}.

DISCUSSION

We feel that the surface chemistry models of CO oxidation presented here provide a more accurate description of the catalytic chemistry of the CO–O_2-supported Pt system than the usual Langmuir–Hinshelwood rate expression does. The most important way the models differ from the usual rate expression is that the models are not constrained by the assumption of adsorption equilibrium for CO. Golchet and White (*2*) showed that CO adsorption equilibrium is not approached in the low C_{CO} regime on Pt metal, where the rate is first order in C_{CO}. Models I and II fit the supported Pt data in Fig. 1 more closely than the Langmuir–Hinshelwood rate expression. In the low C_{CO} regime, the models correctly predict that the rate is approximately first-order in C_{CO} and predict that the surface concentration of CO is much smaller than it would be if CO were in adsorption equilibrium.

Under what reaction conditions is CO adsorption equilibrium approached on the active sites in a supported Pt catalyst? Infrared surface concentration measurements combined with rate measurements should be useful in answering this question provided that diffusional effects and adsorption on inactive sites are accounted for. An infrared-kinetic study using supported Pt (*30*) reported that the surface concentration of CO was very low at gas phase CO concentrations below and at the maximum rate measured and was high at higher gas phase CO concentrations. Diffusional limitations were reported to be present at the

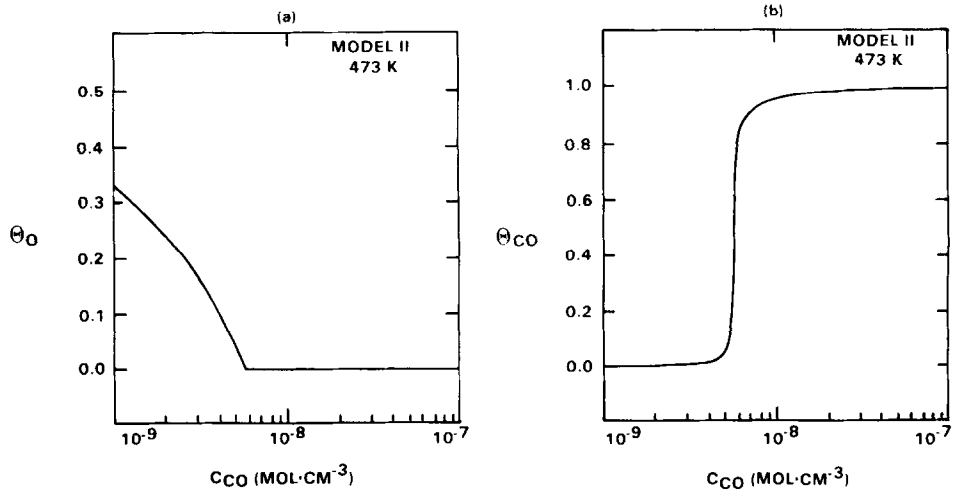

FIG. 5. Model II: Dimensionless surface concentrations of (a) $O_a(\theta_O)$ and (b) $CO_a(\theta_{CO})$ under the reaction conditions of Fig. 4 at 473 K.

lower gas phase CO concentrations, however, making a clear interpretation of these results difficult.

Additional data are required before we can choose between Model I and Model II for a description of CO oxidation on supported Pt. While both models have more parameters than Eqs. (1) and (2), the values of these parameters might be measureable in independent experiments with the catalyst (e.g., thermal desorption experiments).

The adsorption, desorption, and reaction rate parameter values used to fit the supported catalyst data are similar to those determined with unsupported metallic Pt. This similarity suggests that the reaction occurred on reduced, metallic Pt atoms in the supported catalyst. The small value of the parameter α suggests that only a small fraction of the surface Pt atoms in the supported catalyst were in a reduced, active state. This catalyst was given an oxidizing pretreatment (see Table 1) for the purpose of stabilizing its activity. In such a pretreatment, most of the Pt should form an oxide: PtO or PtO_2 (*34*). While oxidized Pt can chemisorb CO (*11*), it is unlikely that it can dissociatively chemisorb O_2. We propose that only a small fraction of the surface Pt atoms in the supported catalyst were in a reduced state and in a grouping with other reduced atoms large enough to catalyst CO oxidation. A similar proposal was made by Boudart *et al.* (*35, 36*) in a comparison of hydrogen oxidation on Pt foils at low pressures with this reaction on silica-supported Pt at high pressures. The most likely reaction mechanism at low pressures also accounted for the observations at high pressures, but the probability of water formation per collision of H_2 with Pt was six orders of magnitude lower on the supported Pt than on the Pt foil. The surfaces of the Pt particles in the supported catalyst were proposed (*36*) to be almost completely covered with "corrosively chemisorbed oxygen," leaving only one site in 10^6 vacant for hydrogen adsorption.

An alternate explanation of the relatively low CO oxidation activity of the supported catalyst would be that all of the surface Pt was active, but adsorption and desorption rate parameters are much smaller for the supported Pt or Pt oxide than for unsupported Pt. The strong adsorption of CO on supported Pt (*37*) and the observation that CO adsorbs with approximately equal strength on oxidized and unoxidized Pt crystal surfaces (*11*) argue against this alternative.

Other studies have demonstrated that the oxidation of Pt reduces its ability to catalyze an oxidation reaction. Gland and Korchak (*38*) studied ammonia oxidation on Pt crystals using mass spectrometry and Auger electron spectroscopy and found that the oxidation reaction was poisoned by surface Pt oxide. Ostermaier *et al.* (*39*) found that the rate of ammonia oxidation on alumina-supported Pt decreased rapidly as the Pt crystallites became oxidized during the reaction. We expect that a supported Pt catalyst in which a large fraction of the Pt is present in a reduced state will have a higher initial activity for CO oxidation than a supported catalyst given an oxidizing pretreatment.

We would like to emphasize the importance of accounting for the effects of diffusional limitations when studying CO oxidation on supported catalysts. Precautions were taken to minimize these limitations in the catalyst considered here: the catalyst contained a small amount of Pt (0.036 wt%), was impregnated with Pt only in a thin outer layer (39 μm), and was subjected to a deactivating pretreatment. Even with these precautions taken, diffusional limitations were present at the lower CO concentrations considered. The almost certain presence of these limitations during CO oxidation at low C_{CO} in supported catalysts complicates the interpretation of any rate multiplicities which might be observed. Rate multiplicities might result from the intrinsic reaction kinetics (e.g., Model I, Fig. 2), and can result from the coupling of diffusional limitations with intrinsic reac-

tion kinetics that by themselves do not exhibit multiplicities (e.g., Eq. (2), Fig. 1 (*32, 33*). Because of this complexity, we feel that the existence of intrinsic CO oxidation rate multiplicities during the steady-state isothermal operation of a supported catalyst has not been clearly demonstrated.

CONCLUSIONS

Reaction models in which CO adsorption equilibrium is not assumed fit CO oxidation rate data more correctly than a Langmuir–Hinshelwood rate expression that assumes adsorption equilibrium. The parameter values used to fit the supported Pt data considered here are similar to those determined with Pt crystals. However, they indicate that CO may be adsorbed less strongly on the supported Pt and that most of the surface Pt atoms in the supported catalyst were deactivated by an oxidizing pretreatment.

APPENDIX 1: NOMENCLATURE

a	Metal area per unit volume in impregnated region of pellet (cm^2 cm^{-3})
a	Subscript denoting adsorbed species
C	Concentration in gas phase (mol cm^{-3})
D	Effective diffusivity of CO in pellet (cm^2 s^{-1})
ΔE	Activation energy (kJ mol^{-1})
F	Frequency of collision of gas phase molecules with metal surface atoms (s^{-1})
K	Equilibrium adsorption constant (cm^3 mol^{-1})
k	Rate constant (dimensions given in text as required)
L	Characteristic diffusion length in pellet (cm)
M	Molecular weight (g g-mol^{-1})
R	Ideal gas constant
Rate	Rate of CO oxidation (dimensions given in text)
Rate_D	Rate of CO oxidation under conditions where diffusional limitations are present
r	Reaction rate (s^{-1})
S	Initial sticking coefficient (dimensionless)
T	Catalyst temperature (K)
T_g	Gas temperature (K)
α	Fraction of surface metal atoms active for the CO oxidation reaction (dimensionless)
β	Parameter describing variation in activation energy for CO desorption with θ_{CO} (kJ mol^{-1})
η	Effectiveness factor (dimensionless)
θ	Surface concentration (dimensionless)
σ	Area occupied by one mole of surface metal atoms (cm^2 mol^{-1})
ϕ	Thiele parameter (dimensionless)

APPENDIX 2: SOLUTION PROCEDURE

In this section we treat the problem of finding steady-state solutions to the system of ordinary differential equations (26) and (28), or (26) and (31), corresponding to various values of the parameter C_{CO}. By setting derivatives equal to zero to model steady-state conditions we obtain a system of nonlinear algebraic equations of the form

$$G(\mathbf{x}, \lambda) = \begin{bmatrix} g_1(\mathbf{x}, \lambda) \\ g_2(\mathbf{x}, \lambda) \\ \cdot \\ \cdot \\ \cdot \\ g_N(\mathbf{x}, \lambda) \end{bmatrix} = \mathbf{0}. \qquad (37)$$

Here $\mathbf{x} = (x_1, \ldots, x_N)^T$ is the vector of unknowns and λ is the scalar parameter. In our examples $N = 2$, $\mathbf{x} = (\theta_{CO}, \theta_O)^T$, and $\lambda =$

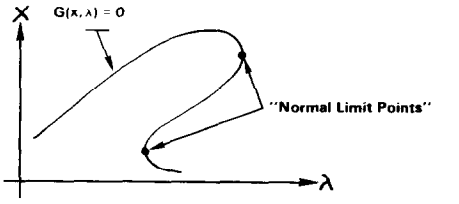

FIG. 6. Solution curve Γ.

C_{CO} (see Eq. (12)). The components of G are the right-hand sides of the differential equations (26) and (28), or (26) and (31).

Solutions to the system (37) may be obtained by straightforward application of Newton iteration coupled to an Euler continuation procedure provided by Jacobian:

$$G_x(\mathbf{x}, \lambda) = \left(\frac{\partial g_i}{\partial x_j}\right) \qquad i,j = 1, \ldots, N \quad (38)$$

is nonsingular over the intended range of λ's. If this is the case, Newton iteration gives a sequence of iterates $(\mathbf{x}_k)$ defined by

$$\mathbf{x}_{k+1} = \mathbf{x}_k - G_x^{-1}(\mathbf{x}_k, \lambda)G(\mathbf{x}_k, \lambda). \quad (39)$$

The sequence $(\mathbf{x}_k)$ converges quadratically to the solution $\mathbf{x}(\lambda)$ of Eq. (37) for a prescribed λ. If we change λ to a new value, say $(\lambda + \Delta\lambda)$, an initial guess for $\mathbf{x}(\lambda + \Delta\lambda)$ may be obtained through an application of a one-step Euler procedure. That is, we select

$$\Delta\mathbf{x} = \frac{d\mathbf{x}}{d\lambda}\Delta\lambda \quad (40)$$

and take $(\mathbf{x} + \Delta\mathbf{x})$ as the initial Newton approximation to $\mathbf{x}(\lambda + \Delta\lambda)$. The derivative $d\mathbf{x}/d\lambda(\lambda)$ may be evaluated by applying the chain rule to Eq. (37) to obtain

$$\frac{d\mathbf{x}}{d\lambda}(\lambda) = -G_x^{-1}\frac{dG}{d\lambda}. \quad (41)$$

In our examples the Jacobian can become singular, evidencing the presence of so-called "normal limit points." These points correspond to places where the solution $\mathbf{x}$, considered as a function of λ, turns back on itself. An illustration in one dimension is given in Fig. 6. Because of possible singularities in the Jacobian we cannot use the Newton–Euler procedure described above directly on the system (37). Instead we must use a continuation procedure developed by Keller (*40*) which is capable of solving the system in the presence of these singularities. The starting point of Keller's procedure is to avoid using the usual parameterization of the solution curve Γ.

$$(\Gamma = \{(\mathbf{x}, \lambda) | G(\mathbf{x}, \lambda) = \mathbf{0}, \lambda \epsilon [\lambda_{\min}, \lambda_{\max}]\}) \quad (42)$$

This standard parameterization gives $\mathbf{x}$ as a function of λ (as depicted in Fig. 6). Instead, Keller treats $\mathbf{x}$ and λ as functions of arc length $\hat{s}$ along Γ, i.e.,

$$\mathbf{x} = \mathbf{x}(\hat{s}) \quad (43)$$

$$\lambda = \lambda(\hat{s}). \quad (44)$$

Mathematically, this amounts to augmenting the system (37) with an equation

$$N(\mathbf{x}, \lambda, \hat{s}) = 0 \quad (45)$$

relating $\mathbf{x}$ and λ to arc length $\hat{s}$. In practice an algebriac function N relating $\mathbf{x}$ and λ to arc length will not be known. However, it is possible to relate $\mathbf{x}$ and λ to a variable s, which is an approximation to true arc length, through a function N derived from the relation

$$\left|\left|\frac{d\mathbf{x}}{d\hat{s}}\right|\right|^2 + \left|\frac{d\lambda}{d\hat{s}}\right|^2 = 1. \quad (46)$$

To obtain the required relationship among the variables $\mathbf{x}$, λ, and s we assume that at some point s_0 the solution is known, say $\mathbf{x} = \mathbf{x}(s_0)$ and $\lambda = \lambda(s_0)$. Then at $s = (s_0 + \Delta s)$ we define

$$N(\mathbf{x}, \lambda, s) = (\mathbf{x}(s) - x(s_0)) \cdot \frac{d\mathbf{x}}{ds}(s_0) + (\lambda(s) - \lambda(s_0))\frac{d\lambda}{ds}(s_0) - \Delta s \quad (47)$$

and approximate Eq. (45) by requiring that

$$N(\mathbf{x}, \lambda, s) = 0. \quad (48)$$

Results in (*40*) establish that the system obtained by appending Eq. (48) to the original system (37) is uniquely solvable at normal limit points, as well as at points where G_x is nonsingular. This result permits the application of Newton–Euler procedure to the inflated system.

We refer the reader to (*40*) and (*41*) for a more detailed description of this procedure.

ACKNOWLEDGMENTS

We are grateful to Edward J. Bissett, GMR Mathe-

matics Department, for suggesting the continuation procedure used in our solution of the surface conservation equations.

REFERENCES

1. Schlatter, J. C., and Chou, T. S., "Measuring CO Oxidation Rates in an External Recycle Reactor," paper 66f, 71st Annual Meeting, AIChE, November 1978.
2. Golchet, A., and White, J. M., *J. Catal.* **53,** 266 (1978).
3. Conrad, H., Ertl, G., and Kuppers, J., *Surface Sci.* **76,** 323 (1978).
4. Engel, T., and Ertl, G., *Adv. Catal.* **28,** 1 (1979).
5. Matsushima, T., *J. Catal.* **55,** 337 (1978).
6. Matsushima, T., *Surface Sci.* **79,** 63 (1979).
7. Gland, J. L., and Korchak, V. N., *Surface Sci.* **75,** 733 (1978).
8. Gland, J. L., *Surface Sci.* **93,** 487 (1980).
9. Fisher, G. B., Sexton, B. A., and Gland, J. L., *J. Vac. Sci. Technol.* **17,** 144 (1980); Gland, J. L., Sexton, B. A., and Fisher, G. B., *Surface Sci.* in press.
10. Chen, M., and Schmidt, L. D., *J. Catal.* **56,** 198 (1979).
11. McCabe, R. W., and Schmidt, L. D., *Surface Sci.* **65,** 189 (1977).
12. Varghese, P., Carberry, J. J., and Wolf, E. E., *J. Catal.* **55,** 76 (1978).
13. Matsushima, T., Almy, D. B., and White, J. M., *Surface Sci.* **67,** 89 (1977).
14. Bonzel, H. P., and Burton, J. J., *Surface Sci.* **52,** 223 (1975).
15. Strozier, J. A., Jr., Cosgrove, G. J., and Fischer, D. A., *Surface Sci.* **82,** 481 (1979).
16. Hopster, H., Ibach, H., and Comsa, G., *J. Catal.* **46,** 37 (1977).
17. Wilson, G. R., and Hall, W. K., *J. Catal.* **17,** 190 (1970).
18. Wilson, G. R., and Hall, W. K., *J. Catal.* **24,** 306 (1972).
19. McCabe, R. W., and Schmidt, L. D., *Surface Sci.* **66,** 101 (1977).
20. Weinberg, W. H., Comrie, C. M., and Lambert, R. M., *J. Catal.* **41,** 489 (1976).
21. Taylor, J. L., Ibbotson, D. E., and Weinberg, W. H., *Surface Sci.* **90,** 37 (1979).
22. Falconer, J. L., and Madix, R. J., *J. Catal.* **48,** 262 (1977).
23. Taylor, J. L., and Weinberg, W. H., *Surface Sci.* **78,** 259 (1978).
24. Madix, R. J., and Benziger, J., *Ann. Rev. Phys. Chem.* **29,** 285 (1978).
25. Beusch, H., Fieguth, P., and Wicke, E., *Chemie. Ing. Technol.* **44,** 445 (1972).
26. Eigenberger, G., 4th Int. Symp. Chem. Reaction Engng., Heidelberg, 1976, paper VII, p. 290.
27. Eigenberger, G., *Chem. Eng. Sci.* **33,** 1255 (1978).
28. Bykov, V. I., and Yablonskii, G. S., *Kinet. Katal.* **18,** 1305 (1977).
29. Bykov, V. I., Yablonskii, G. S., and Kim, U. F., *Doklady Akad. Nauk* **242,** 637 (1978).
30. Cochran, H. D., Donnelly, R. G., Modell, M., and Baddour, R. F., *Colloid Interface Sci.* **3,** 131 (1976).
31. Petersen, E. E., "Chemical Reaction Analysis." Prentice-Hall, Englewood Cliffs, New Jersey, 1965.
32. Wei, J., and Becker, E. R., *ACS Adv. Chem. Ser.* **143,** 116 (1975).
33. Hegedus, L. L., Oh, S. H., and Baron, K., *AIChE J.* **23,** 632 (1977).
34. Yao, H. C., Sieg, M., and Plummer, H. K., Jr., *J. Catal.* **59,** 365 (1979).
35. Boudart, M., Collins, D. M., Hanson, F. V., and Spicer, W. E., *J. Vac. Sci. Technol.* **14,** 441 (1977).
36. Hanson, F. V., and Boudart, M., *J. Catal.* **53,** 56 (1978).
37. Foger, K., and Anderson, J. R., *Appl. Surface Sci.* **2,** 335 (1979).
38. Gland, J. L., and Korchak, V. N., *J. Catal.* **53,** 9 (1978).
39. Ostermaier, J. J., Katzer, J. R., and Manogue, W. H., *J. Catal.* **41,** 277 (1976).
40. Keller, H. B., *in* "Applications of Bifurcation Theory" (P. Rabinowitz, Ed.), p. 359. Academic Press, New York, 1977.
41. Bissett, E. J., and Cavendish, J. C., "A Numerical Technique for the Calculation of Effectiveness Factors in General Situations Displaying Multiplicity," paper 127b, 72nd Annual Meeting, AIChE, November 1979.